JOURNAL OF MATERIALS SCIENCE 20 (1985) 4075–4083

Hardening non-linear behaviour in longitudinal tension of unidirectional carbon composites

TAKASHI ISHIKAWA, MASAMICHI MATSUSHIMA, YOUICHI HAYASHI
First Airframe Division, National Aerospace Laboratory, 1880 Jindaiji, Chofu, Tokyo 182, Japan

Uniaxial tensile tests of unidirectional carbon–epoxy coupons are conducted in the longitudinal direction. It is observed that the longitudinal modulus increases with axial stress or strain up to the intermediate level of tension. A fractional constitutive relation with a quadratic denominator is derived by the method of the theory of non-linear elasticity. This equation adopting the estimated higher-order compliance coefficients exhibits an excellent agreement with the experimental results. An empirical strain-based equation is also proposed as a simpler alternative. Averaging formulae for both types of relation are provided for a practical application. The present phenomenon includes the behaviour in a low-stress region discovered by some early work. The consideration of the present non-linear behaviour improves the correlation between theory and experiments in stress–strain relationships of fabric composites with carbon fibres.

1. Introduction

Plastics reinforced by carbon fibres like carbon–epoxy or carbon–PEEK are showing real promise for super-lightweight aerospace structures. Recent advances in the strengthening of polyacrylonitrile (PAN) fibres may accelerate the development of such structures. Furthermore, engineers in the aircraft industry recognize that the strong anisotropy of these composites contributes to a realistic aeroelastic tailoring technique [1] in wing design. A stringent correlation between theory and experiments is especially required for this new area of technology.

Carbon composites, however, sometimes annoy designers and researchers by the lack of a precise agreement of theory with practice. One of the authors experienced [2] that the predicted longitudinal modulus by the Rule of Mixtures and the corresponding fibre modulus reported by the manufacturer [3] are much higher than measured values at the low strain level ($= 500 \times 10^{-6}$) in the basic part of the aeroelastic tailoring research programme conducted at the National Aerospace Laboratory. This experience provided a motivation for the present paper. The other background is the analysis of the non-linear behaviour of fabric composites conducted serially by the authors. A comparison of theory and experiments [4] suggests to us that unidirectinal (UD) carbon composites must exhibit a non-linear stress–strain behaviour of a hardening type in longitudinal tension. An extensive literature survey also indicates that this suggestion should be true. Curtis *et al.* [5] reported first a dependency of longitudinal modulus of a single carbon fibre on stress, but no quantitative explanation was given there. An empirical formula relating stress and longitudinal modulus of UD carbon composites was proposed by van Dreumel *et al.* [6]. This linear equation, however, has no rational background. Besides both papers confined themselves to the behaviour at lower stress levels. Some other

0022–2461/85 $03.00 + .12

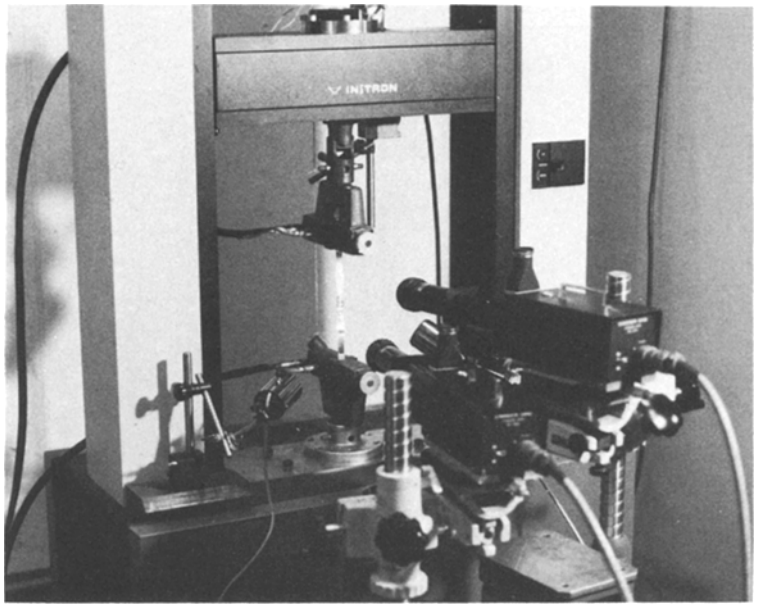

Figure 1 Experimental apparatus.

literature (e.g. [7, 8]) shows hardening non-linear material behaviour of carbon composites unintentionally.

The present paper states first the experimental results of longitudinal tensile tests of carbon–epoxy UD composites where a sophisticated strain-measurement system is utilized. It is confirmed that the stress–strain curves are convex downwards at lower stress levels. A rational constitutive equation is derived next from the theory of non-linear elasticity as a convenient tool for the description of such behaviour. Higher-order elastic compliances are estimated based on the experimental results. An empirical formula relating the longitudinal modulus and strain is also given as an alternative tool for the description.

2. Experimental procedure

Straight coupon-type specimens are cut out of a plate cured with 4-ply UD prepreg tapes of P–3060 (Toray Co.) which consists of T–300 fibres and No. 3601 epoxy resin. The specimen sizes are 350 mm in length, 12.5 mm in width and approximately 0.5 mm in thickness, and the quantity is five. A coincidence of the fibre and coupon directions is fully achieved by a cautious cutting procedure. There should be no fibre waviness and no thermal warping in the specimens. The reason why the warping is undesirable is that the present strain measurement system is highly sensitive to a coupling strain induced by warping.

An Instron model 1125 testing machine is employed here. A pair of electro-optical displacement indicators (Zimmer 100B) are adopted as an extensometer instead of common strain gauges, because strain gauges may stiffen thin coupons and the linearity of the entire circuit can be regarded as insufficient for the present purpose. These electro-optical machines are very accurate, and skills in target-making contribute to an improvement of the accuracy. The gauge length between targets is precisely 100 mm and the grip length 50 mm, so there is plenty of margin from a grip to a target. A quasi-static strain rate of 6.7×10^{-5} is selected. Volume fractions of fibre for the coupons are measured by a burn-out method equivalent to ASTM D2584, and the averaged results of V_f is 69%. Fig. 1 depicts the experimental apparatus.

An example of a direct output of load against strain curves for Specimen No. 3 is shown in Fig. 2, and the scale of stress is also given there. We can see that the curve is convex downwards, particularly up to 60 or 70% of the failure strain. Kamimura *et al.* [8] report similar stress–strain relations even for 0/90 cross-ply laminates where some knee effects are expected. Fukunaga [7] shows more seriously non-linear stress–strain curves. From here on, we define the variable longitudinal elastic modulus $E_L(\sigma_1, \varepsilon_1)$ as a

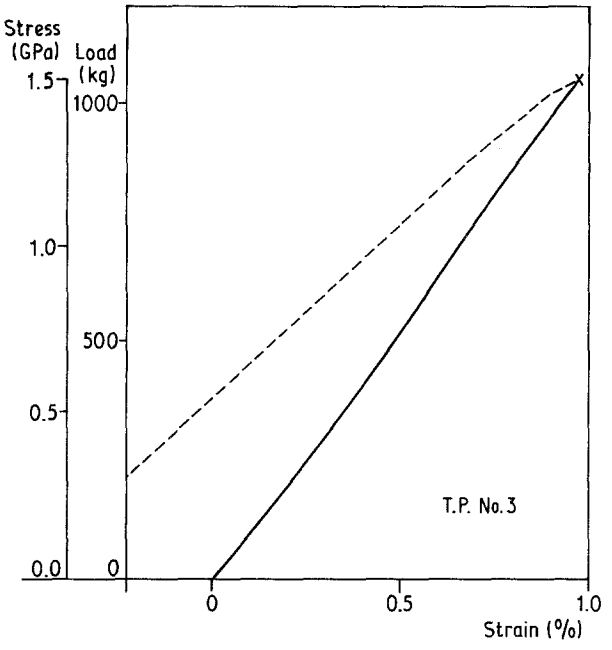

Figure 2 An example of a direct output of a load–strain curve, Specimen No. 3.

derivative of the stress–strain curve, namely

$$E_L(\sigma_1, \varepsilon_1) = d\sigma_1/d\varepsilon_1 \quad (1)$$

where subscript 1 denotes the longitudinal axis. In practice, a finite load increment $\Delta P = 1.57\,\text{kN}$ is chosen as a compromise between the number of load increments and the accuracy of data reduction. Furthermore, the data reduction is started from the load level of $P = 0.392\,\text{kN}$ in order to discard initial fluctuation in the measurement. The relationship between E_L and σ_1 for each specimen obtained from the aforementioned procedure is shown in Fig. 3. Although a scatter in the results is considerable, two clear trends can be recognized: E_L increases at smaller stress levels, and decreases before the final failure.

The averages of the plotted data in Fig. 3 in terms of both E_L and σ_1 are calculated and indicated in Fig. 4. As mentioned previously, van

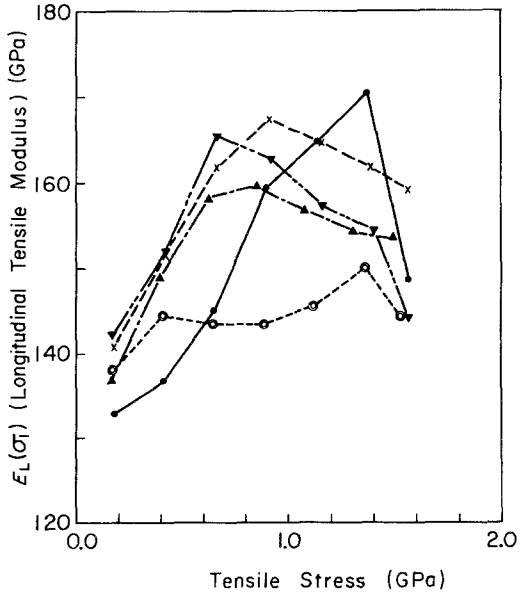

Figure 3 Summary of the experimental relationships between the longitudinal modulus and stress.

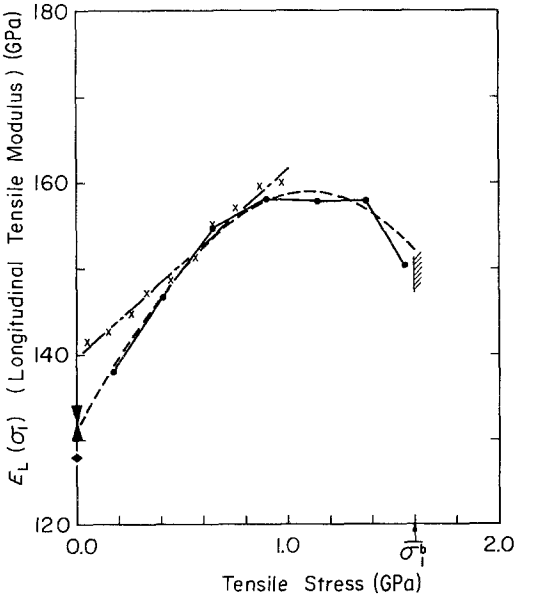

Figure 4 Averages of the results and the fitted fractional constitutive relation. (●) Experimental, (x) from [6], (——) Equation 18.

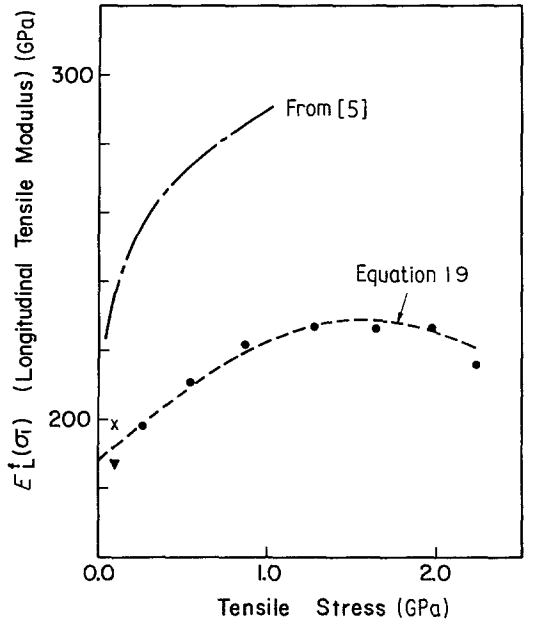

Figure 5 A relationship between the axial fibre modulus and the fibre stress through the Rule of Mixtures: (●) experimental results; (x, ▼) aeroelastically tailored composite wing model [2].

Dreumel and Kamp [6] also describe the hardening behaviour. Their experimental results and their empirical linear formula with respect to stress are also indicated in Fig. 4. Note that their data are truncated at the stress level of 1.0 GPa. A dashed line corresponds to the constitutive equation given later.

Fig. 5 depicts a modified relation between fibre stress σ_1^f and longitudinal fibre modulus E_L^f obtained by the following equations equivalent to the Rule of Mixtures:

$$E_L^f = [E_L - (1 - V_f)E_m]/V_f \quad (2)$$

$$\sigma_1^f = [\sigma_1 - (1 - V_f)E_m\varepsilon_1]/V_f \quad (3)$$

where E_m is assumed to be invariant and equal to 3.92 GPa, and where the average of measured V_f, 69%, is used.

3. Constitutive equations derived from non-linear elasticity

The theory of non-linear elasticity based on complementary energy function W^* was applied to a description of non-linear stress–strain behaviour under a longitudinal shear loading of UD composites by Hahn and Tsai [9] and Hahn [10]. The present non-linear behaviour can be described again by adopting such a manner. One favourable point in the present non-linearity is that loading and unloading paths are precisely identical. The application of the complementary energy function to this case, therefore, seems to be more convincing than to the non-linear shear behaviour where such a good identity of paths is never found. Another favourable point is that an effect of finite deformation can be neglected here because the maximum strain is around 1%.

Following the well-established work by Green and Adkins [11] we can define the strain energy function W for a pure elastic continuum. Stresses are obtained by differentiating W as follows:

$$\partial W/\partial e_{ij} = \sigma_{ij} \quad (i, j = 1, 2, 3) \quad (4)$$

where e_{ij} are tensorial strains. If the following condition holds,

$$\det(\partial^2 W/\partial e_{ij}\partial e_{kl}) \neq 0 \text{ and } > 0 \quad (5)$$

we can define the complementary energy function W^* by

$$W^* = \sigma_{ij}e_{ij} - W \quad (6)$$

For unidirectinal composites, the condition of Equation 5 is valid due to some physical considerations (see Appendix I). By employing W^*, strains are obtained similarly to Equation 4:

$$e_{ij} = \partial W^*/\partial\sigma_{ij} \quad (7)$$

Let us assume that the present UD material is transversely isotropic in the 2–3 plane and that the plane-stress state is appropriate. W^* can then be expanded with polynomial bases σ_1, σ_2 and σ_6^2 [9, 11]. An unabridged expression up to the fourth order of W^* is reached:

$$\begin{aligned} W^* = {} & \underline{\tfrac{1}{2}S_{11}\sigma_1^2} + \tfrac{1}{2}S_{22}\sigma_2^2 + \tfrac{1}{2}S_{66}\sigma_6^2 \\ & + S_{12}\sigma_1\sigma_2 + \underline{\tfrac{1}{3}S_{111}\sigma_1^3} + \tfrac{1}{3}S_{222}\sigma_2^3 \\ & + S_{112}\sigma_1^2\sigma_2 + S_{122}\sigma_1\sigma_2^2 + S_{166}\sigma_1\sigma_6^2 \\ & + S_{266}\sigma_2\sigma_6^2 + \underline{\tfrac{1}{4}S_{1111}\sigma_1^4} + \tfrac{1}{4}S_{2222}\sigma_2^4 \\ & + \tfrac{1}{4}S_{6666}\sigma_6^4 + S_{1112}\sigma_1^3\sigma_2 + S_{1122}\sigma_1^2\sigma_2^2 \\ & + S_{1222}\sigma_1\sigma_1^3 + S_{1166}\sigma_1^2\sigma_6^2 + S_{2266}\sigma_2^2\sigma_6^2 \\ & + S_{1266}\sigma_1\sigma_2\sigma_6^2 \end{aligned} \quad (8)$$

A loading applied in the present experiment is a uniaxial tension and a transverse stress σ_2 will rapidly vanish away from grips. The terms not underlined in Equation 8 can therefore be omitted as follows:

$$W^* = \tfrac{1}{2}S_{11}\sigma_1^2 + \tfrac{1}{3}S_{111}\sigma_1^3 + \tfrac{1}{4}S_{1111}\sigma_1^4 \quad (9)$$

The longitudinal strain ε_1 is given by

$$\varepsilon_1 = \partial W^*/\partial e_{11} = S_{11}\sigma_1 + S_{111}\sigma_1^2 + S_{1111}\sigma_1^3 \tag{10}$$

where the identity between tensorial and engineering strains, $e_{11} = \varepsilon_1$, is considered. Hence, the longitudinal elastic modulus is obtained after the assumption of Equation 1:

$$E_L = \frac{d\sigma_1}{d\varepsilon_1} = \frac{1}{(d\varepsilon_1/d\sigma_1)} = \frac{1}{S_{11} + 2S_{111}\sigma_1 + 3S_{1111}\sigma_1^2} \tag{11}$$

Thus, the dependency of E_L on σ_1 is described by a fractional function of the second order using higher-order elastic compliance coefficients. It should be noted that the pure linear relation, $E_L = 1/S_{11}$, holds when $\sigma_1 = 0$. Another important point is that the empirical equation of van Dreumel and Kamp [6] can be derived from Equation 11. If S_{11}, S_{111} and S_{1111} are the same order of magnitude (as stated later), the following approximation is very common for smaller σ_1:

$$\frac{1}{S_{11} + 2S_{111}\sigma_1 + 3S_{1111}\sigma_1^2} \simeq \frac{1}{S_{11}} - \frac{2S_{111}}{S_{11}^2}\sigma_1 \tag{12}$$

Thus, the linear relation with respect to σ_1 is reached.

4. Estimation of higher-order compliance and discussion

A comparison and fitting of Equation 11 with the experimental data of Fig. 4 provides a determination procedure for the higher-order compliance coefficients. A direct least-squares fitting may be possible but seems too complicated. The following simple sequence is employed instead of a direct method.

By extrapolation of the averaged experimental data, S_{11} is determined as

$$S_{11} = 1/E_L(0) = 7.634 \times 10^{-3}\,\text{GPa}^{-1} \tag{13}$$

Secondly, the axis of symmetry of the second-order fractional function is assumed to be $\sigma_1 = 1.1$ GPa by inspection of Fig. 4. After these two steps, Equation 11 is rewritten by introducing an unknown parameter k:

$$E_L(\sigma_1) = \frac{1000}{7.634 + k\,[(\sigma_1 - 1.1)^2 - 1.21]} \tag{14}$$

A weighted least-squares technique for the inverse of Equation 14 is then adopted, namely

$$\text{minimize: } \sum_{m=1}^{N} W^{(m)} \left[\frac{1}{E_L\sigma_1^{(m)}} - \frac{1}{E_L^{(m)}}\right]^2 \tag{15}$$

where $\sigma_1^{(m)}$ and $E_L^{(m)}$ are the set of the data in Fig. 4 and $W^{(m)}$ is a weighting factor. The reason why the weighting technique is utilized is that fitting at lower stress levels is regarded as more practically important than at higher stress levels. The value of $W^{(m)} = 2$ is chosen for the left-hand four points in Fig. 4, and $W^{(m)} = 1$ for the right-hand three points. A regression equation is derived as

$$\sum_{m=1}^{N} W^{(m)} \left(\frac{7.634 + k\,[(\sigma_1^{(m)} - 1.1)^2 - 1.21]}{1000} - \frac{1}{E_L^{(m)}}\right)[(\sigma_1^{(m)} - 1.1)^2 - 1.21] = 0 \tag{16}$$

By substituting the data in Fig. 4, we obtain $k = 1.111$ and it follows that

$$S_{111} = -1.222 \times 10^{-3}\,\text{GPa}^{-2}$$
$$S_{1111} = 0.3703 \times 10^{-3}\,\text{GPa}^{-3} \tag{17}$$

Hence, Equation 12 is actually written as

$$E_L = 1000/(7.634 - 2.444\,\sigma_1 + 1.111\,\sigma_1^2) = 1000/[6.289 + 1.111\,(\sigma_1 - 1.1)^2]\,\text{GPa} \tag{18}$$

Some discussion will be provided here about the estimated results. Basically, an agreement of Equation 18 plotted by a dashed line in Fig. 4 with the averaged experimental modulus is very favourable. The data from van Dreumel and Kamp [6] fitted by their linear relation is rather similar to the present results up to the intermidiate stress range in trends. This fact is consistent with the theoretical explanation of Equation 12. Equation 13 leads to $E_L(0) = 131$ GPa, and it is worth mentioning that similar values of E_L frequently appear in the literature (e.g. [12–14]). A dashed line in Fig. 5 also represents the following constitutive equation of carbon fibres derived from the same procedure as mentioned above, with the data sets indicated

by dots:

$$E_L^f(\sigma_1^f) = 1000/[4.367 - 1.202\,\sigma_1^f + 0.3803\,(\sigma_1^f)^2] \quad (19)$$

where the unit is GPa. Again, the correlation between the estimated relation and the reduced data is very good. Fig. 5 also shows results of Curtis *et al.* which were measured directly for single fibres by using an ultrasonic technique. Although the absolute values are different from the present results (probably because of the fibre material) we can find an analogous tendency of hardening. Note that the average of these data [5] is close to the value of E_L^f used in some old papers, e.g. Kobayashi and Ishikawa [15], namely $E_L^f = 280$ GPa.

In practice, it seems sometimes to be awkward to apply directly Equations 18 and 19 for UD carbon composites and single carbon fibres because a non-linear calculation is always necessary. An average in the applied stress range from σ_1^0 to σ_1^a is sufficient in many practical cases. Therefore, an averaging formula is worth showing here for the fractional constitutive equation of Equations 18 and 19:

$$\bar{E}_L = \int_{\sigma_1^0}^{\sigma_1^a} \frac{E_L\,d\sigma}{\sigma_1^a - \sigma_1^0} = \frac{\arctan\left(\frac{\sigma_1^a + B}{A}\right) - \arctan\left(\frac{\sigma_1^0 + B}{A}\right)}{3AS_{1111}(\sigma_1^a - \sigma_1^0)} \quad (20)$$

where $A = [(S_{11}/3S_{1111}) - B^2]^{1/2}$ and $B = S_{111}/3S_{1111}$. As an example of an application of this formula to UD composites, $\bar{E}_L = 148$ GPa is obtained in the range from $\sigma_1^0 = 0$ to $\sigma_1^a = 1.0$ GPa, which is 62% of the failure stress.

5. Empirical relation between longitudinal modulus and strain

The relationship between the longitudinal modulus and stress is developed in the previous section. In the actual design process, an expression of the modulus based on strain is required as well. A straightforward substitution of Equation 8 by the strain energy function is as follows:

$$W = \tfrac{1}{2}Q_{11}e_1^2 + \tfrac{1}{2}Q_{22}e_2^2 + \ldots + \tfrac{1}{3}Q_{111}e_1^3 + \ldots Q_{112}e_1^2e_2 + \ldots \quad (21)$$

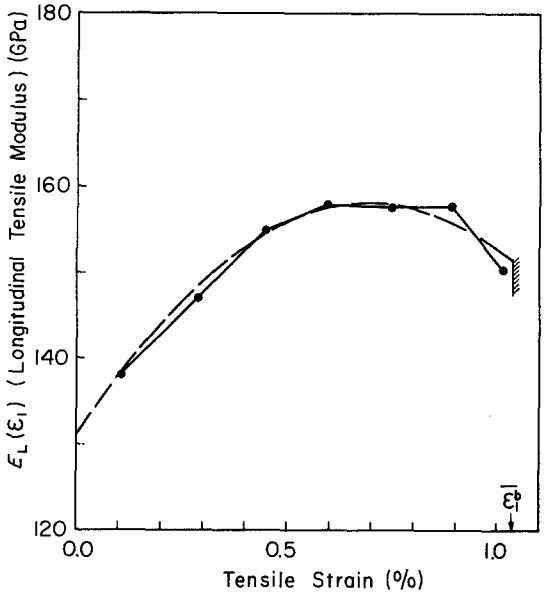

Figure 6 A strain-based description of the present behaviour: (●) experimental results, (——) fitted curve.

However, there lies an obstacle to an employment of the strain energy function W. In a unidirectional tensile test, we produce not only a longitudinal strain e_1 but also transverse strains e_2 and e_3. It follows that many cross-stiffness coefficients of higher order, for example Q_{112}, Q_{113}, Q_{1122}, etc. cannot be omitted for a full description of the present behaviour. It seems, therefore, to be impossible to determine these coefficients only by the uniaxial test.

An empirical relation parallel to the quadratic expression of Equation 21 in form is a possible approach for resolving such an inconvenience. Thus, we have

$$E_L(\varepsilon_1) = E_{L0} + E_{L1}\varepsilon_1 + E_{L2}\varepsilon_1^2 \quad (22)$$

where E_{L1} and E_{L2} are two empirical coefficients which may be referred to as higher-order longitudinal Young's moduli. These two moduli can be estimated similarly to the above-mentioned procedure. The experimental results in Fig. 4 are modified into the relationship between E_L and ε_1 and indicated in Fig. 6. The quadratic relation of Equation 22 is then fitted by using the weighted least-squares technique, and the following results can be reached:

$$E_L(\varepsilon_1) = 131 + 7.71 \times 10^3\varepsilon_1 - 5.51 \times 10^5\varepsilon_1^2 \quad (23)$$

where the relation $E_L(0) = 131$ GPa is

TABLE I Comparison of averaged longitudinal tensile moduli

σ_1 (GPa)	Modulus (GPa)		
	Equation 20	Equation 24	Rule of Mixtures
0	131.0	131.0	159.9
1.0	148.0	148.3	(E_L^f = 230,
1.6 (= σ_b)	151.4	151.2	V_f = 69%)

maintained. As a much simpler tool for practical applications, the average between ε_1^0 and ε_1^a is given here:

$$\bar{E}_L = E_{L0} + \tfrac{1}{2}E_{L1}(\varepsilon_1^a + \varepsilon_1^0) + \tfrac{1}{3}E_{L2}[(\varepsilon_1^a)^2 + \varepsilon_1^a\varepsilon_1^0 + (\varepsilon_1^0)^2] \quad (24)$$

Table I is prepared here in order to compare two values of averages obtained by Equations 20 and 24. The initial point is commonly assumed to be the stress-free state. The results calculated from the Rule of Mixture assume an invariant E_L^f = 230 GPa based on Toray data [3] for T-300/3 K, E_m = 3.92 GPa and V_f = 69%. It can be seen that the two averages are quite similar. The Rule of Mixtures result is rather close to the averages up to the failure stress or strain. This fibre modulus, therefore, is inappropriate as the basic material data for a calculation of elastic response. We can employ such a modulus for a simple material evaluation like a comparison of specific moduli of various filaments. Equation 20 or 24, or an application of Equation 19 with the relevant V_f will provide a much more comprehensive longitudinal modulus in a rigorous structural design.

The compressive behaviour of UD carbon/epoxy still remains unclear at the present stage. By adapting a stress–strain curve in compression shown in a textbook [18], however, an implicative result is obtained as stated in Appendix II. Some more compressive experiments are necessary for a definite conclusion.

6. Example of application of the present consitutive equation

In order to demonstrate the importance and effectiveness of the present constitutive equation, an application is presented here as an example. One of the authors has developed material non-linear analysis of fabric composites [16]. At the level of that work [16], three sources of material non-linearity are taken into account: the first one is behaviour analogous to the knee

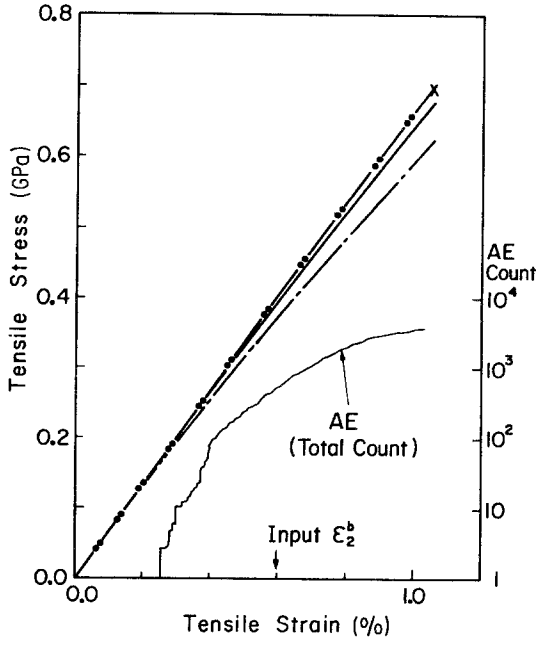

Figure 7 Application of the fractional relation to the theoretical stress–strain analysis of carbon–epoxy composites with a reinforcement of 8H satin fabrics. (● ●) Experimental, (———) FMN, (– – –) PMN.

[17] caused by many transverse crackings, the second one is an off-axis non-linear behaviour [9] related to the thread crimp found in fabric [16], and the third one is a non-linearity in pure resin regions also characteristic of fabric composites. In that paper, non-linear stress–strain relationships of glass–polyimide 8H satin composites are well simulated by the consideration of these three sources.

For the case of carbon–epoxy, however, theoretical results in [16] for 8H satin do not agree with experimental curves [4] to a favourable extent. The cause can be ascribed to the present longitudinal non-linear behaviour of carbon fibres. The constitutive relation of a fractional function, Equation 18, is then added to the process of a non-linear calculation. The work cited [16] should be referred for details of the theoretical part. Fig. 7 depicts a comparison between the fully material non-linear solution including Equation 18 and the partial material non-linear solution of [16], which are abbreviated as FMN and PMN respectively. We can observe that a correlation of the FMN curve with the experimental results of an on-axis tensile test of thick 8H satin carbon–epoxy specimen is very good. The curve labelled AE (Total Count) represents a total count number

measured by an acoustic emission device. This quantity is mainly related to the transverse cracking which is less influential in the case of carbon composites than glass composites because of the difference in the longitudinal moduli. Thus, the non-linear behaviour of the present concern is the most dominant property for a better theoretical description of the stress–strain relationships of the composites with carbon fibres of the present type.

7. Conclusions

(a) A serious dependency of the longitudinal modulus of UD carbon composites on stress or strain is found by uniaxial tensile tests. The longitudinal modulus increases as stress or strain increases up to an intermediate level of tension. Stress–strain curves are convex downwards particularly in such a state.

(b) A fractional constitutive relation with a quadratic denominator is derived based on the theory of non-linear elasticity. Two higher-order compliance coefficients, S_{111} and S_{1111}, are estimated by fitting the constitutive equation to the experimental results. The fractional relation with the estimated coefficients exhibits an excellent agreement with the experimental moduli. An averaging formula for the moduli is given for a convenient practical application.

(c) An empirical relation between the longitudinal modulus and strain is also provided instead of a rational equation. This relation is useful for a strain-based description of the present behaviour.

(d) The longitudinal modulus of a single fibre reported by the manufacturers is close to the average from zero stress up to failure.

(e) A potential of the present equations is demonstrated in an example of a theoretical description of the non-linear stress–strain property of carbon–epoxy composites with a reinforcement of 8H satin fabrics.

Appendix I A Condition for positive definiteness in Equation 9

An elastic continuum must have a positive definite strain energy function W from thermodynamics considerations [19]. On the other hand, it can be concluded that W^* should also be positive and definite. This condition is written as

$$\det\left(\partial^2 W^*/\partial\sigma_{ij}\partial\sigma_{kl}\right) > 0 \qquad \text{(A1)}$$

Because only σ_1 is meaningful in the present case, we have

$$\partial^2 W^*/\partial\sigma_1^2 = S_{11} + 2S_{111}\sigma_1 + 3S_{1111}\sigma_1^2 > 0 \qquad \text{(A2)}$$

The following inequalities are necessary and sufficient in order that Equation A2 holds for the global stress range:

$$S_{1111} > 0, \qquad 3S_{11}S_{1111} - S_{111}^2 > 0 \qquad \text{(A3)}$$

Note that the present higher-order moduli of Equations 13 and 17 satisfy the above condition.

Appendix II A modification of Equation 18 considering compressive behaviour

Some stress–strain curves under an axial compressive loading are available in the literature for typical carbon–epoxy systems. The curve shown in Jones [18] is used here and it is reduced to the relationship between the longitudinal compressive modulus E_L^c and σ_1. The results are depicted in Fig. 8 by open squares. Because the fibre material and V_f of the utilized curve are uncertain, a direct correlation of the present data indicated by dots with those squares may not be suitable from a strict standpoint. Fig. 8, however, gives full confidence for the application of the fractional equation. The solid curve

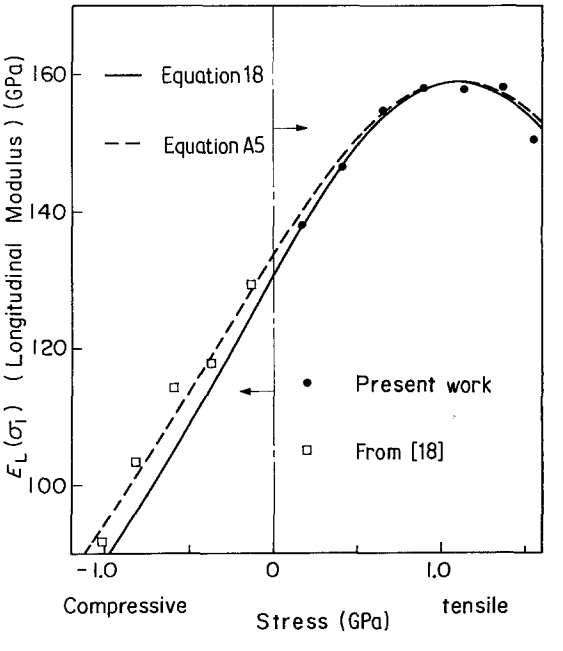

Figure 8 A trial of an extrapolation of the fractional relation into the compression region.

derived from Equation 18 is not far from the compressive moduli, and a slight modification of this equation provides a better fitting in the global range of stress. A weighted least-squares technique similar to Equation 16 with the same peak of the curve as Equation 18, 1000/6.289 at $\sigma_1 = 1.1$, gives us the following coefficients:

$$S_{11} = 7.477 \times 10^{-3} \quad S_{111} = -1.080 \times 10^{-3}$$
$$S_{1111} = 0.3273 \times 10^{-3} \quad \text{(A4)}$$

(units are based on GPa)

It follows that

$$E_L = \frac{1000}{6.689 + 0.982\,(\sigma_1 - 1.1)^2} \quad \text{(A5)}$$

An agreement of this equation (expressed by the dashed curve in Fig. 8) with the moduli on the compression side is very good, with favourable correlation on the tension side as well.

By substituting the values of Equation A4 into Equation 20, we have two kinds of averages for tension and compression:

$$\sigma_1 = 0.0 \quad \text{to } \sigma_1 = 1.6: \quad \bar{E}_L^t = 152.2\,\text{GPa}$$
$$\sigma_1 = -1.0 \text{ to } \sigma_1 = 0.0: \quad \bar{E}_L^c = 113.7\,\text{GPa} \quad \text{(A6)}$$

which are indicated by two arrows in Fig. 8. These averages are consistent with the material data appearing in some literature for a bilinear approximation (e.g. [20]).

Acknowledgements

The authors wish to express their sincere gratitude to those who prepared the specimens in Toray Co. Ltd. They also thank deeply Dr H. Fukunaga of the National Aerospace Laboratory for his assistance in the literature survey, and Messrs K. Ito and Y. Nakajima for their great contribution to the experiments.

References

1. K. ISOGAI, Proceedings of the 21st Aircraft Symposium, Japan Society of Aeronautical and Space Sciences, November 1983, p. 28 (in Japanese).
2. J. NAKAMICHI, Y. NOGUCHI and T. ISHIKAWA, Technical Report of National Aerospace Laboratory, NAL TR-825, July 1984 (in Japanese).
3. Toray Co. Ltd., "Technical Data of Carbon Fibre and Its Composites", CF02R2 (Toray Co. Ltd, Nihonbashi, Tokyo, 1982).
4. T. ISHIKAWA, M. MATSUSHIMA and Y. HAYASHI, Proceedings of the 25th Structure and Strength of Materials Conference, Japan Society of Aeronautical and Space Sciences, July 1983, p. 166, (in Japanese).
5. G. J. CURTIS, J. M. MILNE and W. N. REYNOLDS, *Nature* **220** (1968) 1024.
6. W. H. M. VAN DREUMEL and J. L. M. KAMP, *J. Compos. Mater.* **11** (1977) 461.
7. H. FUKUNAGA, PhD thesis, Tokyo University, 1979 (in Japanese).
8. K. KAMIMURA, B. YOON and F. X. DE CHARENTENAY, Proceedings of 4th International SAMPE European Chapter Conference, October 1983, p. 127.
9. H. T. HAHN and S. W. TSAI, *J. Compos. Mater.* 7 (1973) 102.
10. H. T. HAHN, *ibid.* 7 (1973) 257.
11. A. E. GREEN and J. E. ADKINS, "Large Elastic Deformation and Non-Linear Continuum Mechanics" (Oxford University Press, London, 1960).
12. J. H. STARNES, Jr, N. F. KNIGHT, Jr. and M. ROUSE, Proceedings of the 23rd AIAA Structures, Structural Dynamics and Materials Conference, New Orleans, May 1982, p. 464.
13. T. ISHIKAWA and T.-W. CHOU, *J. Mater. Sci.* **17** (1982) 3211.
14. M. S. ANDERSON and W. J. STROUD, *AIAA J.* **17** (1979) 892.
15. S. KOBAYASHI and T. ISHIKAWA, *Fukugo Zairyo Kenkyu* (Composite Materials and Structures) **3** (1974) 12.
16. T. ISHIKAWA and T.-W. CHOU, *J. Compos. Mater.* **17** (1983) 399.
17. S. W. TSAI, "Strength Characteristics of Composite Materials", NASA Contractor Report CR-224 (1965).
18. R. M. JONES, "Mechanics of Composite Materials" (Scripta, Washington, DC, 1975).
19. Y. C. FUNG, "Foundations of Solid Mechanics", (Prentice-Hall, Englewood Cliffs, NJ, 1965).
20. R. M. JONES, "Stress-Strain Relations for Materials with Different Moduli in Tenions and Compression", AIAA Journal, Vol 15, Jan. 1977, p. 16.

Received 27 November
and accepted 19 December 1984